Free Radical Biology and Medicine 67 (2014) 417–425

Contents lists available at ScienceDirect

Free Radical Biology and Medicine

journal homepage: www.elsevier.com/locate/freeradbiomed

Original Contribution

Seeking the mechanism responsible for fluoroquinolone photomutagenicity: a pulse radiolysis, steady-state, and laser flash photolysis study

Sonia Soldevila [a], M. Consuelo Cuquerella [a], Virginie Lhiaubet-Vallet [a], Ruth Edge [b], Francisco Bosca [a,*]

[a] Instituto Universitario Mixto de Tecnologia Quimica (UPV-CSIC), Universitat Politecnica de Valencia, 46022 Valencia, Spain
[b] Dalton Cumbrian Facility, The University of Manchester, Cumbria CA24 3HA, UK

ARTICLE INFO

Article history:
Received 21 August 2013
Received in revised form
25 November 2013
Accepted 25 November 2013
Available online 4 December 2013

Keywords:
Carcinogenicity
DNA
Fluoroquinolones
Genotoxicity
Photolysis
Photochemistry
Free radicals

ABSTRACT

The mechanism responsible for the remarkable photomutagenicity of fluoroquinolone (FQ) antibiotics remains unknown. For this reason, it was considered worthwhile to study in detail the interactions between DNA and a dihalogenated FQ such as lomefloxacin (LFX; one of the most photomutagenic FQs) and its *N*-acetyl derivative ALFX. Studies of photosensitized DNA damage by (A)LFX, such as formation of DNA single-strand breaks (SSBs), together with pulse radiolysis, laser flash photolysis, and absorption and fluorescence measurements, have shown the important effects of the cationic character of the piperazinyl ring on the affinity of this type of drug for DNA. Hence, the formation of SSBs was detected for LFX, whereas ALFX and ciprofloxacin (a monofluorated FQ) needed a considerably larger dose of light to produce some damage. In this context, it was determined that the association constant (K_a) for the binding of LFX to DNA is ca. 2×10^3 M^{-1}, whereas in the case of ALFX it is only ca. 0.5×10^3 M^{-1}. This important difference is attributed to an association between the cationic peripheral ring of LFX and the phosphate moieties of DNA and justifies the DNA SSB results. The analysis of the transient species detected and the photomixtures has allowed us to establish the intermolecular processes involved in the photolysis of FQ in the presence of DNA and 2′-deoxyguanosine (dGuo). Interestingly, although a covalent binding of the dihalogenated FQ to dGuo occurs, the photodegradation of FQ…DNA complexes did not reveal any significant covalent attachment. Another remarkable outcome of this study was that (A)LFX radical anions, intermediates required for the onset of DNA damage, were detected by pulse radiolysis but not by laser flash photolysis.

Fluoroquinolones (FQs)[1] are molecules formed by a quinolinic main ring and an aminoalkyl substituent. They are widely used as antibacterial agents that develop their pharmacological activity through the inhibition of a bacterial gyrase enzyme (topoisomerase II) involved in the replication and repair of bacterial DNA [1]. During the past years, FQs have received much attention owing to their antitumoral activity [2–6]. In vitro and in vivo studies have confirmed their anti-cancer effects, supported by the reduction in all-cause mortality among cancer patients [7]. The direct FQ antitumor effect has been associated with the inhibition of mammalian deoxyribonucleic acid topoisomerase I, topoisomerase II, and DNA polymerase. Moreover, the genotoxic effects exhibited by FQs in eukaryotic systems are enhanced by UV irradiation [8], which confers on them a potential property as photochemotherapeutic agents. This photoinduced genotoxicity has remarkably been detected in 6,8-dihalogenated FQs such as fleroxacin, BAY y3118, and lomefloxacin (LFX; compound proposed in the literature as a photomutagenic standard, see Chart 1) [9–16]. In this context, a large number of studies concerning the photophysical and photochemical properties of a 6,8-dihalogenated FQ have been carried out during the past few years [12,17–21]. Most of them have shown an unusual photodehalogenation by heterolysis of the strong C_8–halogen bond from their triplet excited states (^{3}FQ) [17–21]. This process leads to the generation of an aryl cation with alkylating properties [17–21]. Therefore, the photoinduced DNA damage has been associated with the reactivity of this intermediate [9,19,21]. This is based on the observation of the quenching of an aryl cation arising from ^{3}LFX photodehalogenation by guanosine monophosphate (dGMP) and the detection of a covalent

Abbreviations: ALFX, *N*-acetyllomefloxacin; CFX, ciprofloxacin; dGMP, 2′-deoxyguanosine 5′-monophosphate; dGuo, 2′-deoxyguanosine; FM, flumequine; FQ, fluoroquinolone; LFX, lomefloxacin; PB, phosphate buffer; SSB, DNA single-strand break.

* Corresponding author. Fax: +34 963877809.
E-mail address: fbosca@itq.upv.es (F. Bosca).

0891-5849/$ - see front matter © 2013 Elsevier Inc. All rights reserved.
http://dx.doi.org/10.1016/j.freeradbiomed.2013.11.027

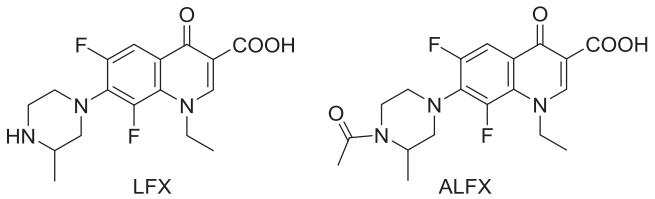

Chart 1. Structure of LFX and its *N*-acetyl derivative ALFX.

binding between LFX and this nucleotide (LFX–dGMP) [21]. However, studies concerning the association of LFX with DNA have revealed that an electron transfer reaction between the singlet excited state of complexed LFX (^{1}LFX…DNA) and DNA must also be involved in the photodehalogenation because, despite the important decrease in LFX emission, the efficiency of this process does not change in the presence of increasing amounts of DNA [22]. Thereby, the literature findings suggest that ^{1}LFX…DNA and ^{3}LFX might be candidates for covalent binding of LFX to DNA.

With this background, the *main processes* involving *LFX photodegradation in the presence of* 2′-deoxyguanosine (*dGuo) or DNA were evaluated by performing* emission studies, laser flash photolysis, pulse radiolysis, and product analysis using ultraperformance liquid chromatography with high-resolution mass spectrometry detection (UPLC–HRMS). In this context, DNA photodamage was assessed through the detection of single-strand breaks in plasmid pBR322 and by examination of the UV–Vis absorption and fluorescence changes in DNA after its photosensitization with FQ and subsequent separation by gel-filtration chromatography to investigate photobinding of LFX to DNA.

Moreover, as it has been established that acetylation of the piperazinyl ring of FQs produces changes in their photophysical and/or photochemical behavior [17,23–25], some key experiments were also performed using the lomefloxacin acetylated derivative 7-(4-acetyl-3-methyl-1-piperazinyl)-1-ethyl-6,8-difluoro-1,4-dihydro-4-oxoquinoline-3-carboxylic acid (ALFX).

Materials and methods

General materials

Calf thymus DNA, ciprofloxacin (CFX), dGuo, flumequine (FM), and LFX were commercial products obtained from Sigma–Aldrich, whereas plasmid pBR322 was supplied by Roche and Sephadex G-25 columns by GE Healthcare. Sodium phosphate buffer (PB) and sodium bicarbonate buffer were prepared from reagent-grade products using Milli-Q water; the pH of the solutions was measured through a glass electrode and adjusted with NaOH to pH 7.4. Other chemicals were of reagent grade and used as received.

The samples of FQs were prepared with various PB concentrations starting from a stock solution of 300 mM PB adjusted to pH 7.4. ALFX was prepared as previously described from a solution of LFX (300 mg, 0.9 mmol) in Ac_2O (50 ml) that was refluxed for 7 h [17]. The solution was cooled to room temperature and concentrated. Afterward, the residue was dissolved in water, neutralized to pH ~7.4, extracted with CH_2Cl_2, and concentrated to dryness.

Absorption and emission measurements

Ultraviolet spectra were recorded on a UV–Vis scanning spectrophotometer (Cary 50). Fluorescence emission spectra were recorded on a Photon Technology International (PTI) LPS-220B fluorimeter. Lifetimes were measured with a time-resolved spectrometer (TimeMaster fluorescence lifetime spectrometer TM-2/2003) from PTI by means of the stroboscopic technique, which is a variation of the boxcar technique. A hydrogen/nitrogen flash lamp (1.8-ns pulse width) was used as excitation source. The kinetic traces were fitted with monoexponential decay functions. Measurements were done under aerated conditions at room temperature (25 °C) in cuvettes of 1-cm path length. The excitation wavelength used to register the fluorescence lifetime was 320 nm. The fluorescence quantum yield of quinine bisulfate in 1N H_2SO_4 (ϕ_F=0.546) was used as standard.

Fluoroquinolone fluorescence quenching by DNA after excitation at 355, 348, and 330 nm was performed using 10^{-4} M FQ buffered aqueous solutions (10^{-3} M PB, pH ~7.4). The DNA concentrations were determined spectrophotometrically taking into account a molar extinction coefficient $\varepsilon_{258\ nm}$=6700 cm^{-1} M^{-1} [22,26]. *Eq.* (1) was selected to determine the drug–DNA interactions from fluorescence quenching data [27–31]:

$$F_0/F = 1 + K_{sv}[Q], \quad (1)$$

where F_0 and F are the fluorescence intensities in the absence and presence of the quencher, respectively; [Q] is the quencher concentration (DNA from 10^{-5} to 1.5×10^{-3} M in nucleotides); and K_{sv} is the Stern–Volmer quenching constant.

Laser flash photolysis experiments

A pulsed Nd:YAG laser was used for the excitation at 355 nm. The single pulses were ~10 ns duration and the energy was from 10 to 1 mJ/pulse. A pulsed xenon lamp was employed as detecting light source. The laser flash photolysis apparatus consisted of the pulsed laser, the Xe lamp, a monochromator, and a photomultiplier made up of a tube, housing, and power supply. The output signal from the oscilloscope was transferred to a personal computer.

Aqueous solutions of 10^{-4} M (A)LFX were prepared in 10^{-3} M $NaHCO_3$ and the experiments registered under anaerobic conditions bubbling N_2O. Transient absorption spectra at different times after the laser pulse were obtained for each sample in the presence and the absence of DNA, paying special attention to intersystem crossing quantum yield changes and to the generation of new intermediates. The DNA concentrations ranged between 10^{-4} and 10^{-2} M in nucleotides.

The quenching experiments were carried out keeping the pH constant at 7.4 throughout the experiment.

Rate constants of aryl cation quenching by biomolecules were determined using the Stern–Volmer Eq. (2):

$$1/\tau = 1/\tau_0 + k[Q]. \quad (2)$$

Pulse radiolysis

The pulse radiolysis experiments were carried out with a 12-MeV Radiation Dynamics Ltd. (UK) 3-GHz electron linear accelerator. We used a single-pulse mode with a pulse duration from 0.22 to 2 μs and with a peak current of about 30 mA. The accelerator is normally operated at 10 pulses per second but the single-pulse mode is achieved by modifying the pulses to the gun [32]. The detection system consisted of a Xe arc lamp and a pulsing unit, high-radiance Kratos monochromator, and quartz optics. Optical transmissions at various wavelengths selected with the monochromator, bandwidths 10 nm, were observed as a function of time before and after the radiation pulse using photoelectric detection. The output of the photomultiplier (EMI 9558Q) was displayed on a Tektronix TDS 380 digitizing oscilloscope. Data processing was performed on a Dan PC using software developed in-house. The sample cell, constructed from Spectrosil quartz, had an optical path length of 25 mm [32].

Deaerated aqueous solutions at pH 7.4 in the presence of 10 mM PB as well as 0.1 M tert-butanol were studied at FQ concentrations (LFX, ALFX, and FM) from 1 to 5×10^{-5} M.

Steady-state photolysis and photoproducts analysis

Photolysis of deaerated aqueous solutions of LFX (10^{-4} M) at pH 7.4 was carried out in the absence and in the presence of 1 mM PB, 10^{-2} M dGuo, as well as DNA (5×10^{-4} M in nucleotides).

Photolysis of (A)LFX was also studied at various PB concentrations (from 1 to 300 mM). Irradiation was performed using a Rayonet photochemical reactor equipped with eight black-light phosphor lamps emitting in the 310–390 nm range, with a maximum at 350 nm [33]. The quantum yields were obtained by comparison with the reported value of 0.6 for LFX [20] photodegradation in water at pH 7.4, which was used as actinometer. All these (A)LFX samples were *aerated and then kept in the darkness for 24 h before analysis to detect stable photoproducts exclusively.*

The photomixtures were analyzed by HPLC with a Spherisorb column (ODS-2, 10 mm packing), an L-6250 intelligent pump, and an L-400 fixed-wavelength UV detector at a wavelength of 325 nm. Acetonitrile/water/trifluoroacetic acid mixtures of 20/79.9/0.1 and 35/64.9/0.1 were used as the mobile phase for LFX and ALFX, respectively. The corresponding photoproducts were identified by UPLC–HRMS. Briefly, the chromatography was performed on an Acquity UPLC system (Waters Corp.) with a conditioned autosampler at 4 °C. The separation was carried out on an Acquity UPLC BEH C18 column (50 × 2.1-mm i.d., 1.7 μm). The column temperature was kept at 40 °C. The analysis was achieved with gradient elution using acetonitrile and water (containing 0.01% formic acid) as the mobile phase. The Waters Acquity XevoQToF spectrometer (Waters Corp.) was connected to the UPLC system via an electrospray ionization (ESI) interface. The ESI source was operated in positive ionization mode with the capillary voltage at 3.0 kV. The temperature of the source and desolvation was set at 100 and 400 °C, respectively. The cone and desolvation gas flows were 100 and 800 L h^{-1}, respectively. All data collected in Centroid mode were acquired using MassLynx software (Waters Corp.). Leucine-enkephalin was used as the lock mass generating an $[M+H]^+$ ion (m/z 556.2771) at a concentration of 500 pg/ml and flow rate of 50 μl/min to ensure accuracy during the MS analysis.

Analysis of LFX photodegradation in the presence of DNA

This study was performed using a 1/1 M ratio of drug/DNA for UV–Vis and fluorescence measurements. LFX was added to DNA (5×10^{-4} M in nucleotides) and allowed to incubate in the dark for 30 min. Samples were then irradiated for various time periods and left in the dark for 30 min.

The drug was separated from the DNA using disposable Sephadex G-25 columns equilibrated with 2/8 ethanol/aqueous 10 mM PB. Controls included drug–DNA mixtures kept in the dark, DNA irradiated or not, and DNA with irradiated drug. The isolated fraction of DNA obtained was analyzed by UV–Vis spectrometry and by fluorescence using three different excitation wavelengths (320, 330, and 350 nm).

Analysis of photoinduced damage to DNA

All the DNA and drug stock solutions were prepared in 1 mM PB. Then, air-equilibrated mixtures containing pBR322 (from 20 μM in base pairs) and LFX, ALFX, or CFX (100 μM) were irradiated using a Luzchem photochemical reactor equipped with six black-light phosphor lamps emitting in the 310–390 nm range, with a maximum at 350 nm [33]. In the case of direct single-strand break (SSB) detection, the loading buffer (0.25% bromophenol blue, 40% sucrose in Milli-Q water) was added immediately after irradiation.

The samples were loaded on a 0.8% agarose gel containing ethidium bromide. After electrophoresis, the relative abundances of supercoiled DNA (form I) and relaxed DNA (form II) were quantified by densitometry (ImageJ).

Results

Emission studies

The binding of (A)LFX to DNA was investigated through fluorescence quenching experiments. With this purpose, aqueous PB solutions of the FQs were prepared and the evolution of their emission spectra in the presence of different DNA quantities was monitored (in Fig. 1, fluorescence spectra and Stern–Volmer plot). Moreover, fluorescence lifetimes of both FQs in the absence and in the presence of DNA (10^{-3} M in nucleotides) were registered to evaluate the possible involvement of a dynamic process in the emission quenching. The data obtained are listed in Table 1.

In agreement with data described in the literature for some FQs including LFX [22], the lifetimes of the LFX and ALFX singlet excited states do not change in the presence of DNA, which discards any dynamic fluorescence quenching process. Therefore, the K_{sv} calculated from Eq. (1) corresponds to the binding constant assuming that the FQ complexed to DNA (FQ…DNA) does not emit. The equilibrium constants for the complex formation were estimated to be ca. 1.9×10^3 M^{-1} for LFX…DNA, a value close to that

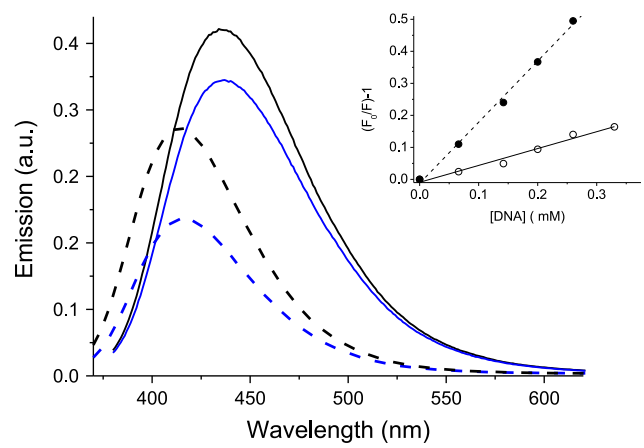

Fig. 1. Emission spectra (λ_{ex}=320 nm) of 10^{-4} M LFX (dashed lines) or ALFX (solid lines) in 10^{-3} M phosphate buffer aqueous solutions, in the absence (black) and in the presence 3.6×10^{-4} M DNA (blue). Inset: Stern–Volmer plots corresponding to the fluorescence quenching of ALFX (open symbols) and LFX (solid symbols) by DNA (circles).

Table 1
Singlet lifetime (τ_F), fluorescence, and photodegradation quantum yields (ϕ_F and ϕ_D, respectively) of LFX and ALFX under various conditions.

	LFX			ALFX		
	τ	ϕ_F	ϕ_D	τ	ϕ_F	ϕ_D
H_2O	1.2	0.080	0.55	1.7	0.110	0.60
1 mM PB	1.1	0.070	0.53	1.7	0.110	0.60
100 mM PB	0.9	0.045	0.50	1.6	0.095	0.58
300 mM PB	0.8	0.033	0.49	1.5	0.088	0.57
0.1 mM DNA (1 mM PB)	1.1	0.052	0.53[a]	1.7	0.105	–
1 mM DNA (1 mM PB)	1.1	0.034	0.53[a]	1.7	0.074	0.59

[a] Ref. [22].

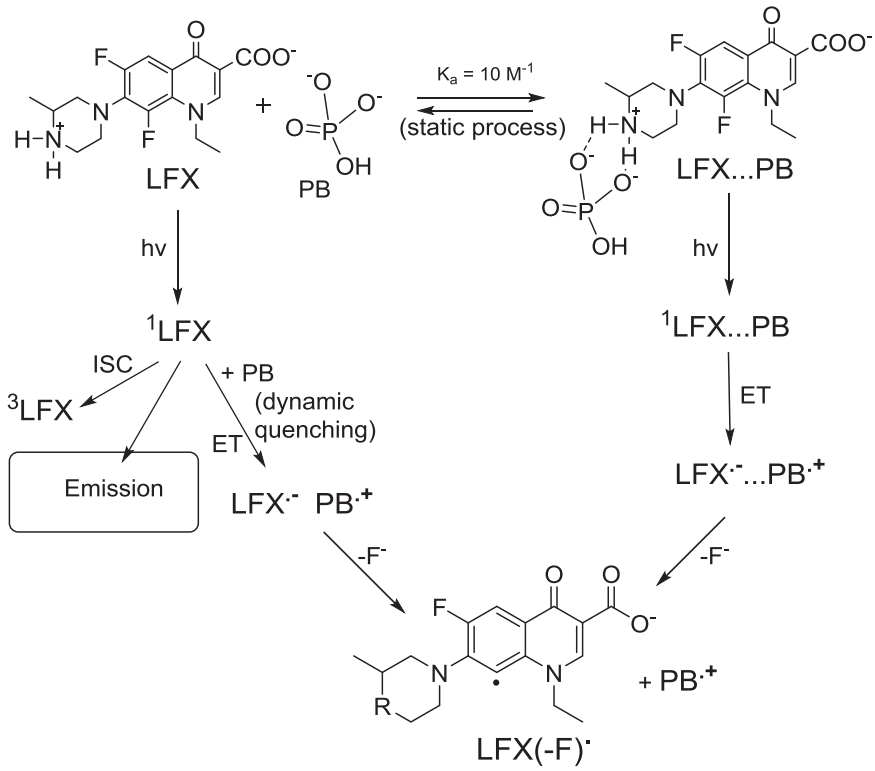

Scheme 1. Mechanisms for LFX fluorescence quenching by phosphate buffer.

reported in the literature [22], and 0.5×10^3 M^{-1} for ALFX…DNA. Hence, N(4′)-acetylation of the piperazinyl ring diminishes the affinity of FQ to DNA, which provides clear evidence that the FQ…DNA association is mainly due to interaction between the cationic piperazinyl ring and the anionic phosphates of the biomolecule backbone. Interestingly, this association can be better understood after analyzing the effects of phosphate buffer on the emission properties of (A)LFX. Hence, fluorescence measurements of these drugs at various PB concentrations (from 1 to 300 mM) revealed that the LFX emission quantum yield decreased more efficiently in the presence of PB than those corresponding to ALFX (see results shown in Table 1).

The LFX emission quenching by PB can be mainly attributed to a static process ($K_a = 10$ M^{-1}) [20] because the small lifetime decrease actually observed accounts for only ca. 15% (dynamic quenching). Scheme 1 shows all pathways involved in the LFX fluorescence quenching by phosphate buffer in which an electron transfer process between PB and the LFX singlet excited state (^{1}LFX…PB) is based on the lack of emission of this complex. The study performed with ALFX substantiates the proposed mechanisms for LFX. Acetylation of the piperazinyl ring prevents ALFX….DNA association; thus, the drop in ALFX emission induced by PB must be related to a dynamic quenching. This process, observed for (A)LFX, turned out to be inefficient because of their very short singlet excited state lifetimes (Table 1).

Laser flash photolysis experiments

Reactivity of (A)LFX aryl cations with dGuo

Photolysis of LFX and ALFX under N_2O at pH 7.4 generates aryl cations of LFX (λ_{max} 490 nm and τ ca. 200 ns) and ALFX (λ_{max} 600 nm and τ ca. 340 ns) [17]. Their reactivity with dGuo was addressed by laser flash photolysis. Fig. 2 shows the transient absorption species detected from LFX aqueous solutions in the presence of dGuo. From the decay traces of the aryl cations maxima were determined for bimolecular rate constants (k_q) of

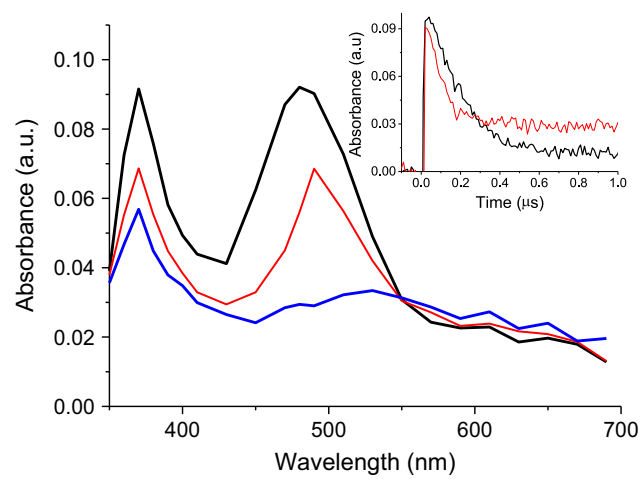

Fig. 2. Transient absorption spectra of 10^{-4} M LFX in aqueous 1 mM $NaHCO_3$ in the presence of 10^{-2} M dGuo, 20 ns (black), 0.10 μs (red), and 0.3 μs (blue) after laser excitation. Inset: decay traces of LFX with and without dGuo (red and black lines, respectively) monitored at 490 nm.

ca. 0.8×10^9 M^{-1} s^{-1} for LFX and 0.3×10^9 M^{-1} s^{-1} for ALFX. Moreover, transient absorption spectra analysis revealed the formation of another intermediate with λ_{max} at 540 nm, which was assigned to dGuo radical by comparison with the literature [34]. The identification of dGuo radical was confirmed by performing similar experiments under aerobic conditions and observing that the transient absorption spectra did not change. Overall, these results are in agreement with the well-known low reactivity of molecular oxygen with aryl cations of (A)LFX [17] as well as with dGuo radical [35]. These data highlight that the electron transfer reaction between the aryl cations of (A)LFX with dGuo occurs efficiently. In this context, the fact that the aryl cation of LFX displays a higher quenching rate constant (k_q) by dGuo than that determined for ALFX aryl cation agrees with the lower reactivity of

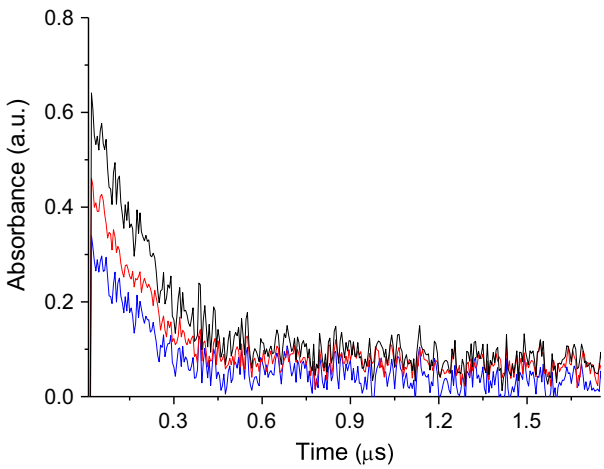

Fig. 3. Decay traces of 1 mM $NaHCO_3$ aqueous solutions upon 355-nm laser excitation of 10^{-4} M LFX (black) with and without 1 and 10×10^{-4} M DNA (red and blue, respectively), at 490 nm.

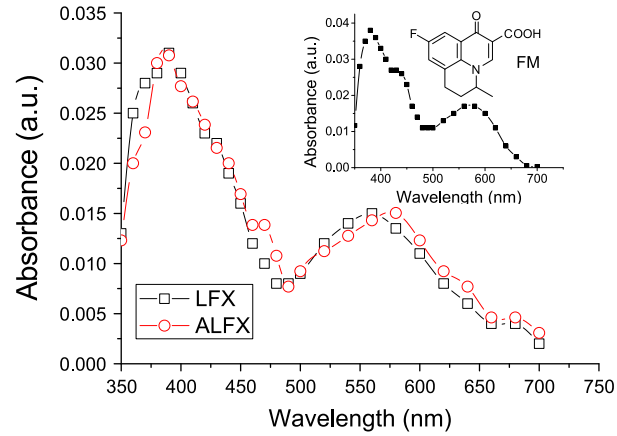

Fig. 4. Transient absorption spectra observed after pulse radiolysis of 5×10^{-5} M ALFX (red circle) and LFX (black square) solution in 10 mM phosphate buffer that contained 1% *t*-BuOH (nitrogen saturated) 5 μs after the irradiation pulse. Inset: transient absorption spectrum observed after pulse radiolysis of 5×10^{-5} M FM under the same conditions at 5 μs after the irradiation pulse.

the latter [17,18]. Interestingly, a k_q of ca. $3 \times 10^9\ M^{-1}\ s^{-1}$ has been reported in the literature for LFX aryl cation quenching by guanosine monophosphate [21]. The increase in the k_q value for the nucleotide with respect to that for the nucleoside can be attributed to some preassociation of the nucleotide phosphate moiety with FQ, as suggested for phosphate buffer [24].

Photoreactivity of (A)LFX with DNA

Laser excitation of (A)LFX (10^{-4} M) in $NaHCO_3$ solutions (10^{-4} M, pH ~7.4) under N_2O atmosphere displayed the same intermediates with similar lifetimes in the absence and the presence of DNA (up to 1.5×10^{-3} M in nucleotides), indicating that the k_q should be $< 10^7\ M^{-1}\ s^{-1}$ for LFX and ALFX aryl cations. However, the generation of these intermediates decreased when DNA was added, this change being more significant in the case of LFX than for ALFX. Thus, as can be observed in the decay traces of Fig. 3, the transient absorption of LFX aryl cation monitored at its λ_{max} decreases in the presence of increasing amounts of DNA. Interestingly, considering the DNA–drug equilibrium,

then

$$K_a = [FQ\ldots DNA]/([DNA] \times [FQ]) \quad (3)$$

Applying the K_a determined above by fluorescence quenching in Eq. (3), and taking into account the initial concentration of FQ and DNA in the LFX experiments, the increase in complexed drug is coincident with the decrease in the generation of the corresponding aryl cations.

One-electron reduction

The reaction of the hydrated electron (e^-_{aq}) with FQ was studied by subjecting a nitrogen-saturated aqueous solution of FQs containing 1% *tert*-butanol (*t*-BuOH) to pulse radiolysis. Under these conditions, the $^{\bullet}OH$ radicals are scavenged by *t*-BuOH to form relatively unreactive free radicals. In the absence of FQ, the absorption due to e^-_{aq} decayed with a first-order rate of $1.0 \times 10^5\ s^{-1}$, and this rate increased to ca. $6 \times 10^5\ s^{-1}$ in the presence of 5×10^{-5} M FQ. Under these conditions the rate of decay of the hydrated electron monitored at 720 nm was found to increase linearly with FQ concentration. The hydrated electron reacts very efficiently with FQ ground state in a diffusion-controlled manner with a bimolecular rate constant of ca. $10^{10}\ M^{-1}\ s^{-1}$ for the three compounds. The transient absorption spectrum of each FQ under these conditions is shown in Fig. 4. Thus, they display the same two bands centered at ca. 560 and ca. 390 nm. The decay of these transient species showed rate constants of k=5.81, 4.5, and $11.5 \times 10^3\ s^{-1}$ for FM, LFX, and ALFX, respectively, at 5×10^{-5} M concentration of each FQ. On the basis of these results, the detected intermediates can be assigned to FQ radical anion ($FQ^{\bullet -}$). In fact, the transient absorption spectrum obtained for FM, a related fluoroquinolone, is similar to that described in the literature for its radical anion [36], and those obtained for (A)LFX are quite similar to radical anions of monofluorated FQ such as norfloxacin or CFX [37].

Kinetic studies and photoproduct analysis of LFX photodegradation

The photophysical studies of LFX were complemented by photoproduct analysis to obtain a better understanding of the intermediates involved in the photolysis of LFX in the presence of biomolecules such as DNA or dGuo. The final aim was to establish the pathways involved in the generation of the covalent linkages between LFX and the biomolecules. Therefore, irradiation of LFX in deaerated solutions (pH ~7.4) was performed with a multilamp photoreactor at λ_{max} 350 nm with and without DNA, dGuo, or PB to consider the influence of the previously proposed electron transfer reaction between ^1FQ and PB or DNA [22,38].

Analysis of the photodegradation in PB monitored by HPLC and UPLC–HRMS unveiled that LFX photoproduct distribution depended on PB concentration. In the absence of PB, irradiation of the sample led only to LFX1 [39], whereas in the presence of PB concentrations up to 300 mM PB, LFX2 [40] and LFX3 [40] generation arose and only traces of LFX1 were found (Scheme 2) [40]. In addition, the presence of PB does not change significantly the LFX photodegradation quantum yield (ϕ_D, Table 1), which cannot be correlated with the drop in LFX fluorescence quantum yields induced by its presence (Table 1).

When LFX irradiation (1 mM PB at pH ~7.4) was carried out in the presence of 5×10^{-4} M DNA, again LFX1, LFX2, and LFX3 were formed. In addition, the photoproduct LFX4 [39] was detected.

In the LFX photodegradation in the presence of dGuo (10 mM, see Scheme 2), in addition to leading to LFX1, LFX2, LFX3, and LFX4, three new compounds absorbing at 350 nm (indicating that they also contain the fluoroquinolone chromophore) and displaying exact masses (*m*/*z*) of 599.2384, 599.2380, and 599.2386, were detected. Based on these results, these isomers can be assigned to LFX–dGuo adducts owing to the theoretical MH^+ of 599.2378 calculated for $C_{27}H_{32}FN_8O_7$ (Scheme 2). By contrast, formation of adducts between DNA and LFX was not detected when the

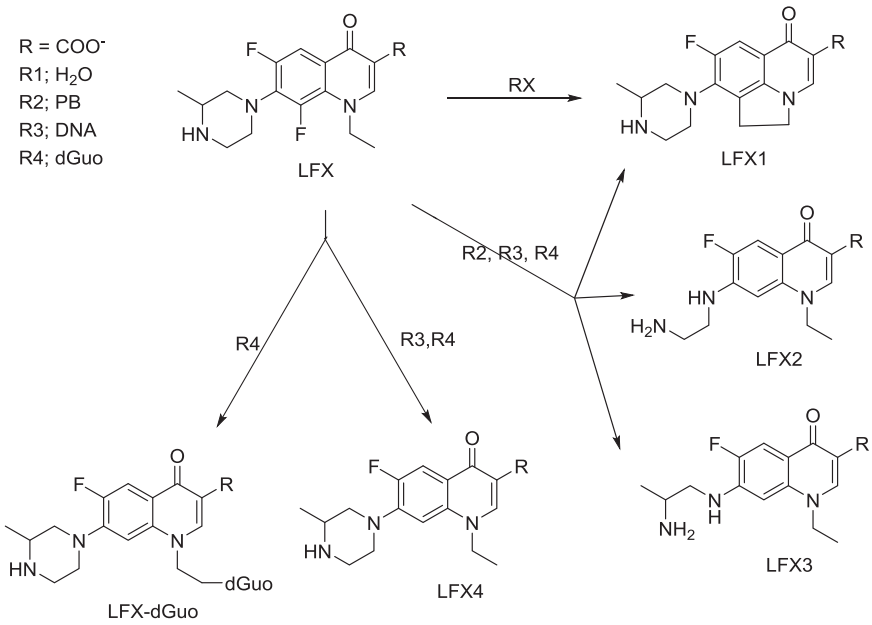

Scheme 2. Photoproducts of LFX obtained after irradiation of aqueous solutions with and without PB, DNA, or dGuo.

corresponding photomixture was analyzed by UV–Vis spectrometry after gel filtration with Sephadex. The filtered DNA-containing samples did not show any change in their absorption spectra and no emission was detected at the excitation wavelengths of 320, 330, and 350 nm.

Another important key outcome was that the presence of PB or DNA did not produce important changes in the photodegradation quantum yield of (A)LFX (Table 1).

Damage to photosensitized DNA

The DNA-photosensitizing properties of (A)LFX and CFX, as a model of monohalogenated FQs, were investigated. The experiments were carried out on supercoiled circular DNA (pBR322), which is known to be a very useful tool to detect various types of damage. Conversion of the supercoiled form (also called form I) into the circular form (or form II), indicative of SSB formation, can be observed directly. Thus, UVA irradiation of pBR322 (20 μM in base pairs) in the presence of the FQ (100 μM) was carried out. As shown in Fig. 5, only LFX induced a significant formation of form II. In this context, 70% of DNA cleavage was observed for LFX after 240 mJ/cm^2 light dose. This value is remarkably higher than those obtained for the ALFX and the monohalogenated CFX, which were 5 and 15%, respectively. The lower DNA damage observed for ALFX can be attributed to a lower FQ…DNA association constant (K_a). In the case of CFX, the lower DNA damage can be associated with a lower photodegradation quantum yield [16] because the K_a of CFX…DNA (2.2×10^3 M^{-1}, determined in this work) is very similar to that of LFX.

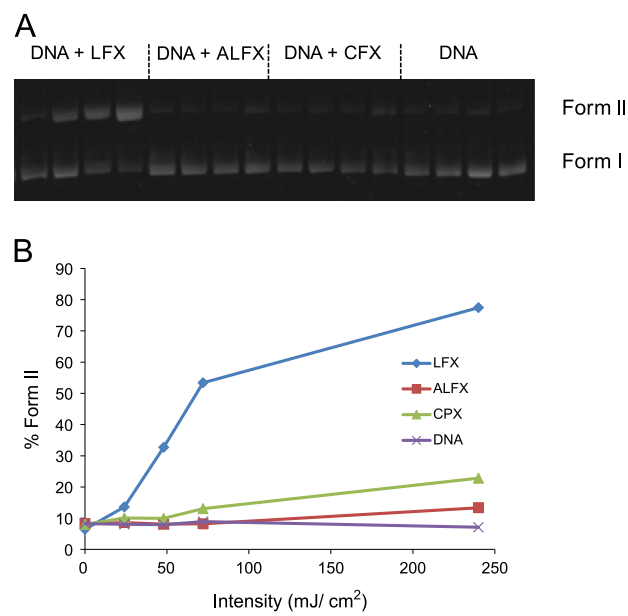

Fig. 5. (A) Agarose gel showing DNA form I (supercoiled native form) and form II obtained from mixtures containing pBR322 (20 μM) and FQ (100 μM) after various light doses (24, 48, 72, 240 mJ/cm^2). (B) Percentage of form II versus light dose for each sample.

Discussion

The irradiation of LFX, its N-acetylated form ALFX, and CFX in the presence of supercoiled circular DNA (pBR322) has revealed that LFX is able to photosensitize DNA damage more efficiently than the dihalogenated ALFX or the monohalogenated CFX (Fig. 5). To understand the obtained results, it is necessary to take into account the FQ mechanisms previously proposed to generate DNA damage:

(a) the alkylating properties of FQ aryl cations generated from photodehalogenation of ^{3}FQ [21];
(b) the oxidative damage by a radical pathway occurring from the intramolecular reaction of the complex ^{1}FQ….DNA [22];
(c) the oxidative damage mediated by the singlet oxygen generated [16,41];
(d) the thymine cyclobutane dimers generated by energy transfer reactions [23,41].

Mechanisms (c) and (d) are involved in most of the FQs, whereas (a) and (b) have been mainly attributed to dihalogenated FQs [16,42]. In this context, photodehalogenation of FQs, more efficient in 6,8-dihalogenated FQs, has been shown to be the most important pathway involved in the photoinduced DNA damage [16,42]. Thus, this effect has been correlated with the photostability of mono- and dihalogenated FQ [16], which explains the low

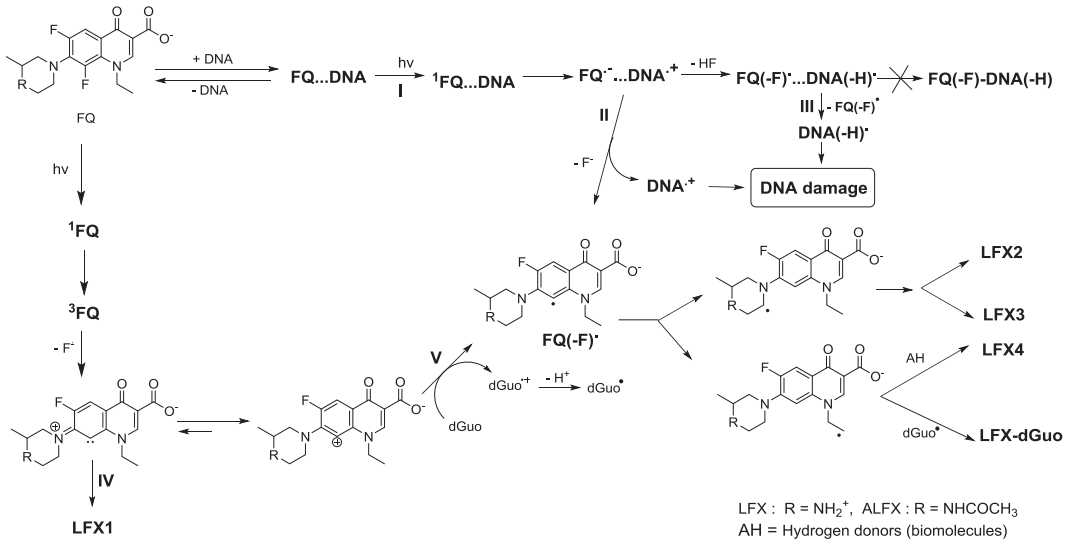

Scheme 3. Main processes of (A)LFX photodegradation involved in dGuo and DNA damage.

DNA damage observed for CFX. However, the differences obtained between LFX and ALFX cannot be easily understood on this basis because the photodehalogenation quantum yield of ALFX is very similar to that described for LFX (Table 1) and the photochemical behaviors of LFX and ALFX in neutral aqueous medium are quite similar [17]. Therefore, it was necessary to evaluate in depth all the processes involved in the photolysis of (A)LFX in the presence of DNA.

Scheme 3 displays all the main processes involved in the photochemistry of (A)LFX in the presence of DNA and of one of its nucleosides (dGuo).

Determination of (A)LFX fluorescence lifetimes, which do not change in the presence of DNA, evidenced that the emission drop was produced by static quenching. In this context, association constants (K_a) of ca. 2×10^3 and. $0.5 \times 10^3\ M^{-1}$ were determined for the LFX…DNA and ALFX…DNA complex formation, respectively. An electron transfer between the quinolinic ring and DNA (path I, Scheme 3), as previously suggested [22], explains these results. This process is also similar to that observed between ^{1}LFX and PB (Scheme 1). The influence of the cationic character of the piperazinyl ring on the affinity of these drugs to DNA has been highlighted by ALFX not only by fluorescence measurements (inset, Fig. 1) but also by laser flash photolysis (Fig. 3). Hence, the higher affinity of LFX to DNA in comparison with ALFX is unequivocally due to an association between the cationic peripheral ring of LFX and the phosphate moieties of the DNA backbone.

The UV–Vis spectrum and fluorescence measurements of the DNA aqueous solutions obtained after the irradiation of LFX with DNA at 5×10^{-4} M concentration (when 40% of LFX was complexed to DNA) and subsequent purification by Sephadex did not show any evidence of a quinolone ring attached to DNA, which discards the formation of covalent binding between (A)LFX and the biomolecule as the main pathway to produce DNA damage. Thus, electron transfer occurring between ^{1}FQ and DNA generates the corresponding FQ radical anion and a nucleoside radical cation; however, hole hopping of the DNA positive charge away from the drug radical anion [43] prevents formation of a covalent bond (see pathways II and III in Scheme 3). Further support for this hypothesis was found when LFX irradiation was performed in the presence of dGuo, in which LFX–dGuo adducts were detected when the nucleoside was not part of the DNA structure (see pathway V). In this case, a dehalogenated radical of LFX (LFX($-$F)$^\bullet$) links to the dGuo radical. Formation of LFX2 and LFX3 during irradiation in the presence of dGuo or DNA is also mediated by LFX ($-$F)$^\bullet$, a radical that it is also generated by LFX photolysis in the presence of PB (see Schemes 2 and 3). The detection of LFX1, as described in the literature [17], arises from an intramolecular reaction of the carbene generated from the free LFX triplet excited state (pathway IV).

The results obtained studying the reactivity of (A)LFX aryl cation with dGuo by the laser flash photolysis technique revealed quenching rate constants of the same order of magnitude for both intermediates (k_q of ca. $0.8 \times 10^9\ M^{-1}\ s^{-1}$ for LFX and $0.3 \times 10^9\ M^{-1}\ s^{-1}$ for ALFX). In this context, an electron transfer between the aryl cations and dGuo generates radical (A)LFX($-$F)$^\bullet$ and dGuo radical cation (dGuo$^\bullet$, see Fig. 2 and pathway V). The key intermediates (A)LFX(F)$^\bullet$ were not detected because they are too reactive to be observed on a nanosecond time scale [44].

Interestingly, although the intermolecular reaction between ^{1}LFX and DNA should generate their corresponding radical ions (pathway I), none of these intermediates were detected by laser flash photolysis. However, LFX$^{\bullet-}$ was detected by pulse radiolysis. This fact would be attributed to the generation of two different conformational isomers of LFX$^{\bullet-}$ (see Scheme 4). The one detected by pulse radiolysis comes from the addition of an electron to the LFX ground state and ought to be more stable than that obtained from electron transfer between DNA and ^{1}LFX. In this case, as a rehybridization accompanied by intramolecular charge transfer (RICT) has occurred in the singlet excited state of the FQ [38], the N(1) of the piperazinyl ring shares electrons with the quinolonic ring, which increases its dehalogenation and, thus, reduces its lifetime. This would also justify the LFX radical anion generated from the ground state displaying an absorption spectrum similar to those of ALFX and FM, which has no piperazinyl ring (Fig. 4). On the other hand, DNA radical cation was not detected because of the delocalization of the radical cation in duplex DNA as discussed above [43].

We also analyzed the possibility that the (A)LFX triplet excited state complexed to DNA defluorinates and then accepts one electron from DNA, or first accepts the electron and subsequently releases F^-. However, the fact that the increase in complexed drug detected by fluorescence was coincident with the decrease in the generation of the corresponding aryl cations excludes both pathways (see Figs. 1 and 3 for LFX). Therefore, as shown in Scheme 3, all the (A)LFX results are in favor of pathways II and III as the main processes to produce DNA damage. Reactions between the DNA radicals (DNA$^\bullet$) or radical cations (DNA$^{\bullet+}$) can explain the DNA dimerization [19], and the reactivity of these intermediates with

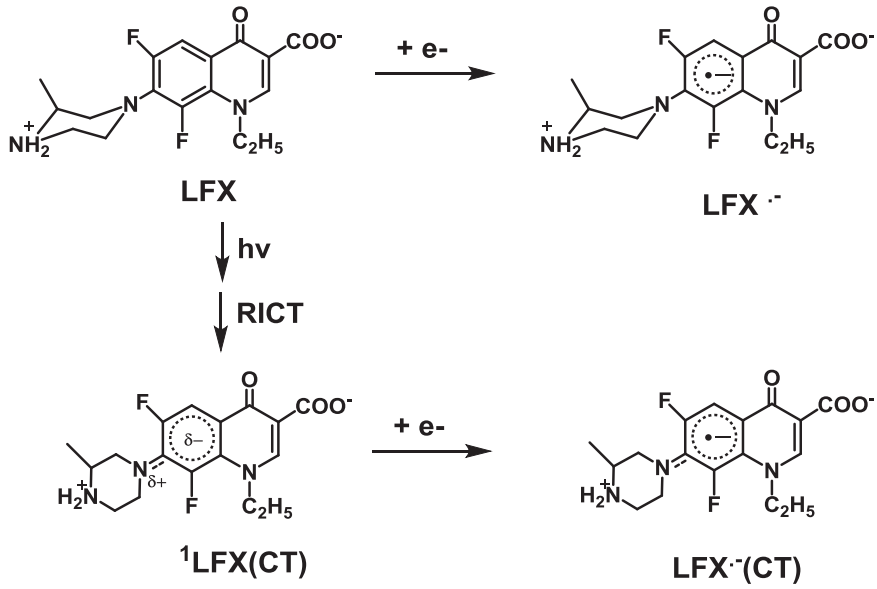

Scheme 4. Generation of LFX radical anions from its ground and singlet excited state.

molecular oxygen justifies the generation of 8-oxo-7,8-dihydro-2′-deoxyguanosine as the most important oxidative DNA damage detected [16]. Hence, the efficient defluorination of (A)LFX complexed to DNA (see Table 1), which occurs through an electron transfer between the singlet excited state of (A)LFX and DNA, is the key process in the generation of the DNA damage by dihalogenated FQs. By contrast, monohalogenated FQs complexed to DNA have an ineffective dehalogenation process [22] and therefore this type of drug needs a longer irradiation time to produce detectable DNA damage as shown in Fig. 5 for CFX and described in the literature for other FQs [16]. In this way, our results are further support for the generation of DNA oxidative damage by the type I process (via radical) in the photolysis of dihalogenated fluoroquinolones, whereas in monohalogenated FQs this type of damage occurs by the type II process (via singlet oxygen) [16]. The fact that most of the LFX-mediated DNA damage was produced at light doses lower than 72 mJ/cm^2 could be associated with the high photolability of this drug. Indeed, under these conditions, LFX should be mostly photolyzed, and SSBs formed at higher irradiation doses should be photoinduced through a type II process by its monohalogenated photoproduct.

The difference in the association constant between LFX… DNA and ALFX… DNA is the main explanation for the low ability of ALFX to produce DNA damage (Fig. 5) because the percentage of DNA complexed with LFX is more than 16%, whereas, using ALFX, this is lower than 4%.

Conclusions

The results of this study support the main photodegradation pathway of dihalogenated FQs, such as LFX and ALFX, to produce DNA damage as being intermolecular electron transfer between the (A)LFX singlet excited state and DNA in the (A)LFX… DNA complex, generating the corresponding radical ions. Hence, as ALFX has an association constant about four times lower than that obtained for LFX, photolysis of this acetylated derivative induces a smaller amount of single-strand breaks. It has been observed that the photodehalogenation of (A)LFX in the presence of dGuo produces formation of a covalent adduct, but interestingly, the generation of the same intermediates in the photodegradation of (A)LFX in the presence of DNA does not display any covalent association.

The present data encourage the development of new mammalian DNA topoisomerase blockers as chemotherapeutic agents. Therefore, by changing fluoroquinolone substituents, it is possible to modulate not only their pharmacological properties but also their affinity for biomolecules and their photosensitizing properties.

Acknowledgment

We thank Professor Suppiah Navaratnam for his help. We acknowledge the Spanish government for Grants CTQ2010-19909 and CTQ2012-32621 and the Generalitat Valenciana for Grants PROMETEOII/2013/005.

References

[1] Domagala, J. M.; Hanna, L. D.; Heifetz, C. L.; Hutt, M. P.; Mich, T. F.; Sanchez, J. P.; Solomon, M. New structure–activity-relationships of the quinolone antibacterials using the target enzyme: the development and application of a DNA gyrase assay. *J. Med. Chem.* **29:**394–404; 1986.
[2] Kang, D. H.; Kim, J. S.; Jung, M. J.; Lee, E. S.; Jahng, Y.; Kwon, Y.; Na, Y. New insight for fluoroquinophenoxazine derivatives as possibly new potent topoisomerase I inhibitor. *Bioorg. Med. Chem. Lett.* **18:**1520–1524; 2008.
[3] Azema, J.; Guidetti, B.; Dewelle, J.; Le Calve, B.; Mijatovic, T.; Korolyov, A.; Vaysse, J.; Malet-Martino, M.; Martino, R.; Kiss, R. 7-((4-Substituted)piperazin-1-yl) derivatives of ciprofloxacin: synthesis and in vitro biological evaluation as potential antitumor agents. *Bioorg. Med. Chem.* **17:**5396–5407; 2009.
[4] Cullen, M.; Baijal, S. Prevention of febrile neutropenia: use of prophylactic antibiotics. *Br. J. Cancer* **101:**S11–S14; 2009.
[5] Kim, K.; Pollard, J. M.; Norris, A. J.; McDonald, J. T.; Sun, Y. L.; Micewicz, E.; Pettijohn, K.; Damoiseaux, R.; Iwamoto, K. S.; Sayre, J. W.; Price, B. D.; Gatti, R. A.; McBride, W. H. High-throughput screening identifies two classes of antibiotics as radioprotectors: tetracyclines and fluoroquinolones. *Clin. Cancer Res.* **15:**7238–7245; 2009.
[6] Al-Trawneh, S. A.; Zahra, J. A.; Kamal, M. R.; El-Abadelah, M. M.; Zani, F.; Incerti, M.; Cavazzoni, A.; Alfieri, R. R.; Petronini, P. G.; Vicini, P. Synthesis and biological evaluation of tetracyclic fluoroquinolones as antibacterial and anticancer agents. *Bioorg. Med. Chem.* **18:**5873–5884; 2010.
[7] Paul, M.; Gafter-Gvili, A.; Fraser, A.; Leibovici, L. The anti-cancer effects of quinolone antibiotics? *Eur. J. Clin. Microbiol. Infect. Dis.* **26:**825–831; 2007.
[8] Perrone, C. E.; Takahashi, K. C.; Williams, G. M. Inhibition of human topoisomerase II alpha by fluoroquinolones and ultraviolet a irradiation. *Toxicol. Sci.* **69:**16–22; 2002.
[9] Lhiaubet-Vallet, V.; Bosca, F.; Miranda, M. A.; Photosensitized, D. N. A. damage: the case of fluoroquinolones. *Photochem. Photobiol.* **85:**861–868; 2009.
[10] Marrot, L.; Belaidi, J. P.; Jones, C.; Perez, P.; Riou, L.; Sarasin, A.; Meunier, J. R. Molecular responses to photogenotoxic stress induced by the antibiotic

lomefloxacin in human skin cells: from DNA damage to apoptosis. *J. Invest. Dermatol.* **121:**596–606; 2003.
[11] Meunier, J. R.; Sarasin, A.; Marrot, L. Photogenotoxicity of mammalian cells: a review of the different assays for in vitro testing. *Photochem. Photobiol.* **75:**437–447; 2002.
[12] Martinez, L. J.; Li, G.; Chignell, C. F. Photogeneration of fluoride by the fluoroquinolone antimicrobial agents lomefloxacin and fleroxacin. *Photochem. Photobiol.* **65:**599–602; 1997.
[13] Chignell, C. F.; Haseman, J. K.; Sik, R. H.; Tennant, R. W.; Trempus, C. S. Photocarcinogenesis in the Tg.AC mouse: lomefloxacin and 8-methoxypsoralen. *Photochem. Photobiol.* **77:**77–80; 2003.
[14] Fasani, E.; Profumo, A.; Albini, A. Structure and medium-dependent photodecomposition of fluoroquinolone antibiotics. *Photochem. Photobiol.* **68:**666–-674; 1998.
[15] Jeffrey, A. M.; Shao, L.; Brendler-Schwaab, S. Y.; Schluter, G.; Williams, G. M. Photochemical mutagenicity of phototoxic and photochemically carcinogenic fluoroquinolones in comparison with the photostable moxifloxacin. *Arch. Toxicol.* **74:**555–559; 2000.
[16] Spratt, T. E.; Schultz, S. S.; Levy, D. E.; Chen, D.; Schluter, G.; Williams, G. M. Different mechanisms for the photoinduced production of oxidative DNA damage by fluoroquinolones differing in photostability. *Chem. Res. Toxicol.* **12:**809–815; 1999.
[17] Albini, A.; Monti, S. Photophysics and photochemistry of fluoroquinolones. *Chem. Soc. Rev.* **32:**238–250; 2003.
[18] Soldevila, S.; Bosca, F. Photoreactivity of fluoroquinolones: nature of aryl cations generated in water. *Org. Lett.* **14:**3940–3943; 2012.
[19] Cuquerella, M. C.; Miranda, M. A.; Bosca, F. Generation of detectable singlet aryl cations by photodehalogenation of fluoroquinolones. *J. Phys. Chem. B* **110:**6441–6443; 2006.
[20] Freccero, M.; Fasani, E.; Mella, M.; Manet, I.; Monti, S.; Albini, A. Modeling the photochemistry of the reference phototoxic drug lomefloxacin by steady-state and time-resolved experiments, and DFT and post-HF calculations. *Chem. Eur. J.* **14:**653–663; 2008.
[21] Fasani, E.; Manet, I.; Capobianco, M. L.; Monti, S.; Pretali, L.; Albini, A. Fluoroquinolones as potential photochemotherapeutic agents: covalent addition to guanosine monophosphate. *Org. Biomol. Chem.* **8:**3621–3623; 2010.
[22] Sortino, S.; Condorelli, G. Complexes between fluoroquinolones and calf thymus DNA: binding mode and photochemical reactivity. *New J. Chem.* **26:**250–258; 2002.
[23] Bosca, F.; Lhiaubet-Vallet, V.; Cuquerella, M. C.; Castell, J. V.; Miranda, M. A. The triplet energy of thymine in DNA. *J. Am. Chem. Soc.* **128:**6318–6319; 2006.
[24] Cuquerella, M. C.; Andreu, I.; Soldevila, S.; Bosca, F. Triplet excimers of fluoroquinolones in aqueous media. *J. Phys. Chem. A* **116:**5030–5038; 2012.
[25] Cuquerella, M. C.; Bosca, F.; Miranda, M. A. Photonucleophilic aromatic substitution of 6-fluoroquinolones in basic media: triplet quenching by hydroxide anion. *J. Org. Chem.* **69:**7256–7261; 2004.
[26] Son, G. S.; Yeo, J. A.; Kim, M. S.; Kim, S. K.; Holmen, A.; Akerman, B.; Norden, B. Binding mode of norfloxacin to calf thymus DNA. *J. Am. Chem. Soc.* **120:**6451–-6457; 1998.
[27] Ahmad, B.; Parveen, S.; Khan, R. H. Effect of albumin conformation on the binding of ciprofloxacin to human serum albumin: a novel approach directly assigning binding site. *Biomacromolecules* **7:**1350–1356; 2006.
[28] Chi, Z. X.; Liu, R. T.; Zhang, H. Noncovalent interaction of oxytetracycline with the enzyme trypsin. *Biomacromolecules* **11:**2454–2459; 2010.
[29] Alarcon, E.; Edwards, A. M.; Aspee, A.; Moran, F. E.; Borsarelli, C. D.; Lissi, E. A.; Gonzalez-Nilo, D.; Poblete, H.; Scaiano, J. C. Photophysics and photochemistry of dyes bound to human serum albumin are determined by the dye localization. *Photochem. Photobiol. Sci.* **9:**93–102; 2010.
[30] Catalfo, A.; Calandra, M. L.; Renis, M.; Serrentino, M. E.; De Guidi, G. Rufloxacin-induced photosensitization in yeast. *Photochem. Photobiol. Sci.* **6:**181–189; 2007.
[31] Alarcon, E.; Maria Edwards, A.; Aspee, A.; Borsarelli, C. D.; Lissi, E. A. Photophysics and photochemistry of rose bengal bound to human serum albumin. *Photochem. Photobiol. Sci.* **8:**933–943; 2009.
[32] Lorenzo, F.; Navaratnam, S.; Edge, R.; Allen, N. S. Primary photoprocesses in a fluoroquinolone antibiotic sarafloxacin. *Photochem. Photobiol.* **85:**886–894; 2009.
[33] Cuquerella, M. C.; Bosca, F.; Miranda, M. A.; Belvedere, A.; Catalfo, A.; de Guidi, G. Photochemical properties of ofloxacin involved in oxidative DNA damage: a comparison with rufloxacin. *Chem. Res. Toxicol.* **16:**562–570; 2003.
[34] Candeias, L. P.; Steenken, S. Ionization of purine nucleosides and nucleotides and their components by 193-nm laser photolysis in aqueous solution: model studies for oxidative damage of DNA. *J. Am. Chem. Soc.* **114:**699–704; 1992.
[35] Steenken, S. Purine bases, nucleosides, and nucleotides: aqueous solution redox chemistry and transformation reactions of their radical cations and e− and OH adducts. *Chem. Rev* **89:**503–520; 1989.
[36] Bazin, M.; Bosca, F.; Marin, M. L.; Miranda, M. A.; Patterson, L. K.; Santus, R. A laser flash photolysis and pulse radiolysis study of primary photochemical processes of flumequine. *Photochem. Photobiol.* **72:**451–457; 2000.
[37] Zhang, P.; Song, X.; Li, H.; Yao, S.; Wang, W. Transient species of several fluoroquinolones and their reactions with amino acids. J. *Photochem. Photobiol. A* **215:**191–195; 2010.
[38] Cuquerella, M. C.; Miranda, M. A.; Bosca, F. Role of excited state intramolecular charge transfer in the photophysical properties of norfloxacin and its derivatives. *J. Phys. Chem. A* **110:**2607–2612; 2006.
[39] Fasani, E.; Negra, F. F. B.; Mella, M.; Monti, S.; Albini, A.; Photoinduced, C.–F. bond cleavage in some fluorinated 7-amino-4-quinolone-3-carboxylic acids. *J. Org. Chem.* **64:**5388–5395; 1999.
[40] Fasani, E.; Mella, M.; Monti, S.; Albini, A. Unexpected photoreactions of some 6-fluoro-7-aminoquinolones in phosphate buffer. *Eur. J. Org. Chem.* **2001 (2):**391–397; 2001.
[41] Sauvaigo, S.; Douki, T.; Odin, F.; Caillat, S.; Ravanat, J. L.; Cadet, J. Analysis of fluoroquinolone-mediated photosensitization of 2′-deoxyguanosine, calf thymus and cellular DNA: determination of type-I, type-II and triplet–triplet energy transfer mechanism contribution. *Photochem. Photobiol.* **73:**230–237; 2001.
[42] Martinez, L.; Chignell, C. F. Photocleavage of DNA by the fluoroquinolone antibacterials. *J. Photochem. Photobiol. B* **45:**51–59; 1998.
[43] Liu, C. S.; Hernandez, R.; Schuster, G. B. Mechanism for radical cation transport in duplex DNA oligonucleotides. *J. Am. Chem. Soc.* **126:**2877–2884; 2004.
[44] Scaiano, J. C.; Stewart, L. C. Phenyl radical kinetics. *J. Am. Chem. Soc.* **105:**3609–3614; 1983.